Comparative Analysis of Different Approaches for Theoretical Simulation of Ultracentrifuge Isotopic Separation Cascades

CÉLIA CHRISTIANI PASCHOA PORTOGHESE* and
CLÁUDIO RODRIGUES

INSTITUTO DE PESQUISAS ENERGÉTICAS E NUCLEARES (IPEN)
TRAVESSA R, 400 - CEP 05508-900, SÃO PAULO, SP, BRAZIL

ABSTRACT

In order to simulate a real cascade performance in terms of the external and internal flow rates and isotopic compositions, it is necessary to solve a system of equations composed of the internal mass balances for the element (U) and for the desired isotopes. Considering the separation of a binary isotopic mixture for a cascade with n stages, we have a system of $4n$ independent equations with $6n$ unknowns. This kind of system has infinite solutions unless we introduce practical or theoretical new equations describing the centrifuge separation performance and/or use approximations in terms of restrictions to the stages behavior. Depending on the equations and/or restrictions we use, the simulation results can be quite different. Six different combinations of theoretical equations and stage restrictions are analyzed and compared in this paper using experimental results in order to establish the best mathematical model for the theoretical simulation of a real cascade performance.

Key Words. Isotopic separation; Ultracentrifugation; Cascade simulation

INTRODUCTION

An ultracentrifuge is a separation device that, when fed with a stream composed of an isotopic mixture, produces two other streams: the product, enriched in the isotopes with lower molecular weights, and the tails, enriched in the isotopes with higher molecular weights.

* To whom correspondence should be addressed.

715

The main characteristic of the ultracentrifugation process is a high level of separation in only one stage, but with low throughput.

In the design of a plant to produce enriched uranium, the amount of material to be produced and the isotopic compositions to be achieved are specified. In order to obtain material with the specified isotopic compositions, ultracentrifuges are connected in series, composing separation stages. In order to produce the amount of material specified, ultracentrifuges are connected in parallel in each stage. This complete arrangement is known as an isotopic separation cascade. The separation stages are interconnected in such a way that the feed stream of a generic Stage i is composed of the product stream of Stage $i - 1$ mixed with the tails stream of Stage $i + 1$.

Normally, the design of an uranium enrichment cascade intended to perform a given separation task in terms of product composition and quantity is also intended to minimize the operational costs. If the material to be processed is a binary mixture, this results in a cascade profile as similar as possible to the ideal one (1), with an established tails composition. Other optimization criteria may be used in cascade design (2–4), but they will not be considered in this paper because of the lack of experimental results.

Simulation of the real behavior of a cascade depends on knowing the characteristic ultracentrifuge curves relating the separative parameters and the flow and pressure variables. By using these curves and the criteria for maximizing the installed separative capacity for a given product and tails compositions, we can obtain a flow distribution in which some ultracentrifuges can operate very close to the optimal point while others can operate far from this same point.

However, by using theoretical relations and/or restrictions to the stages' behaviors, we can achieve results similar to these without knowing the real curves cited above. This level of information is sufficient for starting a cascade design.

Six different possible kinds of approximation for use in the theoretical calculations of internal flow and composition distributions will be compared in this paper with experimental results in order to establish the best method for theoretical cascade simulation.

EQUATIONS AND RESTRICTIONS

To establish the flow rate and isotopic composition of all the internal streams of a given cascade, we have to solve a system composed of the following fundamental equations.

1: Material balance for the U compound in each stage (n equations):

$$F_i = P_i + W_i \tag{1}$$

where F_i, P_i, and W_i are, respectively, the feed, product, and tails flow rates.

2: Material balance for the desired isotope (^{235}U) in each stage (n equations):

$$F_i z_i = P_i y_i + W_i x_i \tag{2}$$

where z_i, y_i, and x_i are, respectively, the feed, product, and tails ^{235}U weight percentage.

3: Material balance for the U compound in the streams mixing points (n equations):

$$F_1 = W_2$$
$$F_i = P_{i-1} + W_{i+1} + \delta_{i,f} F_c, \qquad \text{for } i = 2, \ldots, n-1 \tag{3}$$
$$F_n = P_{n-1}$$

where F_c is the cascade feed flow rate and $\delta_{i,f}$ is equal to 1 for the feed stage, and 0 for the others.

4: Material balance for the desired isotope in the streams mixing points (n equations):

$$F_1 z_1 = W_2 x_2$$
$$F_i z_i = P_{i-1} y_{i-1} + W_{i+1} x_{i+1} + \delta_{i,f} F_c z_f, \qquad \text{for } i = 2, \ldots, n-1 \tag{4}$$
$$F_n z_n = P_{n-1} y_{n-1}$$

where z_f is the ^{235}U weight percentage in the feed material.

Introducing into these equations the concepts of cut (θ_i), heads separation factor (β_i), and tails separation factor (γ_i):

$$\theta_i = P_i / F_i \tag{5}$$
$$\beta_i = R_{pi} / R_{fi} = y_i (1 - z_i) / [z_i (1 - y_i)] \tag{6}$$
$$\gamma_i = R_{fi} / R_{wi} = z_i (1 - x_i) / [x_i (1 - z_i)] \tag{7}$$

where R_{fi}, R_{pi}, and R_{wi} are, respectively, the feed, product, and tails ^{235}U abundance ratios. They can be transformed into the following relations:

$$P_i = \theta_i F_i, \qquad i = 1, \ldots, n \tag{8}$$
$$W_i = (1 - \theta_i) F_i, \qquad i = 1, \ldots, n \tag{9}$$
$$\theta_i = \frac{(\gamma_i - 1)[1 + z_i(\beta_i - 1)]}{\beta_i \gamma_i - 1}, \qquad i = 1, \ldots, n \tag{10}$$

$$F_1 - (1 - \theta_2)F_2 = 0 \tag{11}$$

$$-\theta_{i-1}F_{i-1} + F_i - (1 - \theta_{i+1})F_{i+1} = \delta_{i,f}F_c, \qquad i = 2, \ldots, n-1$$

$$-\theta_{n-1}F_{n-1} + F_n = 0$$

$$F_i z_i - (1 - \theta_2)F_2 x_2 = 0 \tag{12}$$

$$-\theta_{i-1}F_{i-1}y_{i-1} + F_i z_i - (1 - \theta_{i+1})F_{i+1}x_{i+1} - \delta_{i,f}F_c z_f = 0,$$
$$i = 2, \ldots, n-1$$

$$-\theta_{n-1}F_{n-1}y_{n-1} + F_n z_n = 0$$

$$y_i = \frac{\beta_i z_i}{1 + z_i(\beta_i - 1)}, \qquad i = 1, \ldots, n \tag{13}$$

$$x_i = \frac{z_i}{\gamma_i - z_i(\gamma_i - 1)}, \qquad i = 1, \ldots, n \tag{14}$$

The ideal cascade (1) is defined as the cascade arrangement that minimizes the total internal flow rate and, consequently, the power consumption. The ratio between the calculated flow rate per stage and the optimal feed flow rate of one ultracentrifuge (G) gives the number of centrifuges in each stage. In this case all the ultracentrifuges operate in the same optimal flow and separation conditions, which means the same feed flow rate, cut (symmetric), and heads and tails separation factors $(\beta = \gamma)$ that maximize the ultracentrifuge separative power, defined as:

$$\delta U = \left[\theta \frac{R_p - 1}{R_p + 1} \ln R_p + (1 - \theta) \frac{R_w - 1}{R_w + 1} \ln R_w - \frac{R_f - 1}{R_f + 1} \ln R_f \right] * G * \frac{238}{352} \tag{15}$$

In the real case, however, it is not possible to maintain all those variables at the optimal point because we have to round the calculated numbers of centrifuges per stage to integer values and, at the same time, respect the mass balance equations described above.

In order to simulate the real cascade behavior, we can add to this system of equations the following restrictions based on the ideal cascade behavior:

Constant cut for all stages
Symmetric separative behavior for all stages $(\beta = \gamma)$
Constant separation factor $(\alpha = \beta * \gamma)$ for all stages
Constant separative power for all stages

The symmetric separative behavior of one ultracentrifuge can be established using theoretical relations to calculate the heads and tails separation factors. The solution of the diffusion-convection equation in the internal cen-

trifuge field gives the following equations for β and γ (5):

$$\beta = \frac{C_1 + \theta G}{\theta G + C_1 \exp[-(C_1 + \theta G)z_s/C_5}$$ (16)

$$\gamma = \frac{C_1 \exp\{[C_1 - (1 - \theta)G]z_s/C_5\} - (1 - \theta)G}{C_1 - (1 - \theta)G}$$ (17)

where z_c and z_s are related to the feed flow rate introduction position, and C_1 and C_5 are theoretical parameters that can be written as functions of the centrifuge efficiency (e) and its components (5) e_C, e_F, and e_I:

$$C_1 = \frac{\sqrt{2}\Delta M}{2RT} \pi\rho D\omega^2 a^3 \sqrt{\frac{e_F e_C}{1 - e_C}} = b \sqrt{\frac{e/e_I}{1 - e_C}}$$ (18)

$$C_5 = \pi a^2 \rho D(1 + m^2) = C_5' \frac{1}{1 - e_C}$$ (19)

The three efficiency components can be calculated by assuming a theoretical internal flow profile (2). An alternative procedure to estimate these components without the assumption of a theoretical internal flow profile is to consider that the component e_I reaches its maximum value in the optimal separation conditions (G_{ot}, α_{ot}, θ_{ot}, δU_{ot}, or e_{ot}). For these conditions the centrifuge operates in a symmetric process (1) for which the following equations are valid:

$$\beta_{ot} = \frac{b\sqrt{\dfrac{e/e_I}{1 - e_C}} + \theta_{ot}G_{ot}}{\theta_{ot}G_{ot} + b\sqrt{\dfrac{e/e_I}{1 - e_C}}\exp\left[-\left(b\sqrt{\dfrac{e/e_I}{1 - e_C}} + \theta_{ot}G_{ot}\right)\dfrac{z_c(1 - e_C)}{C_5'}\right]}$$ (20)

$$\gamma_{ot} = \frac{b\sqrt{\dfrac{e/e_I}{1 - e_C}}\exp\left[\left(b\sqrt{\dfrac{e/e_I}{1 - e_C}} - (1 - \theta_{ot})G_{ot}\right)\dfrac{z_s(1 - e_C)}{C_5'}\right] - (1 - \theta_{ot})G_{ot}}{b\sqrt{\dfrac{e/e_I}{1 - e_C}} - (1 - \theta_{ot})G_{ot}}$$ (21)

$$\alpha_{ot} = \beta_{ot} * \gamma_{ot}$$ (22)

TABLE 1
Percentage Relative Deviation between Calculated Values and Experimental Results

Mathematical model	Cascade	dR_p (%)	dR_w (%)	dP/F (%)	$d\Delta U$ (%)
1	1	1.5228	−1.1666	−1.7003	5.6400
	2	3.2483	−1.7838	−1.5481	7.0963
	3	−0.2841	0.4127	−0.5487	−1.9951
	4	−11.7699	2.7833	8.0844	−11.5752
	Average	−1.8207	0.0614	1.0718	−0.2085
	Standard deviation	6.7878	2.0367	4.7029	8.5627
	Confidence interval	−12.6200 < d < 8.6786	−3.1791 < d < 3.3019	−6.4104 < d < 8.5540	−13.8318 < d < 13.4148
2	1	0.8549	0.1296	−1.7003	0.7669
	2	1.1774	0.1049	−1.5481	0.3535
	3	−0.1997	0.4127	−0.5487	−1.8450
	4	−6.0826	−0.3976	8.0844	−1.0285
	Average	−1.0625	0.0624	1.0718	−0.4383
	Standard deviation	3.3980	0.3370	4.7029	1.2120
	Confidence interval	−6.4687 ≤ d ≤ 4.3438	−0.4737 ≤ d ≤ 0.5985	−6.4104 < d ≤ 8.5541	−2.3665 ≤ d ≤ 1.4900
3	1	1.5228	−1.1666	−1.7003	5.6035
	2	3.1300	−1.7838	−1.3546	7.0073
	3	−1.1280	0.4127	0.6859	−2.0806
	4	−12.7361	2.5845	9.6661	−11.6479
	Average	−2.3028	0.0117	1.8243	−0.2794
	Standard deviation	7.1737	1.9487	5.3328	8.5672
	Confidence interval	−13.7161 ≤ d ≤ 9.1105	−3.0887 ≤ d ≤ 3.1121	−6.6603 ≤ d ≤ 10.3089	−13.9098 ≤ d ≤ 13.3510

4	1	0.5878	−0.1944	−1.1109	0.6834
	2	0.0533	−0.3148	0.4838	0.2114
	3	−1.1842	0.2162	0.9602	−1.8458
	4	−1.0980	0.1988	0.8787	−0.9620
	Average	−0.4103	−0.0236	0.3030	−0.4783
	Standard deviation	0.8723	0.2714	0.9652	1.1444
	Confidence interval	$-1.7981 \leq d \leq 0.9776$	$-0.4553 \leq d \leq 0.4082$	$-1.2327 \leq d \leq 1.8387$	$-2.2991 \leq d \leq 1.3425$
5	1	2.7251	1.7498	−6.1891	1.3991
	2	6.6209	1.7838	−10.7886	0.9555
	3	16.5087	2.3777	−20.0274	−1.5960
	4	18.4453	2.3857	−20.7381	−1.4074
	Average	11.0750	2.0743	−14.4358	−0.1622
	Standard deviation	7.6028	0.3553	7.1250	1.5592
	Confidence interval	$-1.0210 \leq d \leq 23.1710$	$1.5091 \leq d \leq 2.6395$	$-25.7717 \leq d \leq -3.0999$	$-2.6429 \leq d \leq 2.3185$
6	1	0.7213	−0.1944	−1.2242	1.6180
	2	0.6449	−0.5247	0.0968	1.4796
	3	−0.3685	0.0197	0.4152	−0.9801
	4	1.2297	−0.1988	−0.8787	0.9681
	Average	0.5569	−0.2246	−0.3987	0.7714
	Standard deviation	0.6693	0.2246	0.7776	1.2007
	Confidence interval	$-0.5079 \leq d \leq 1.6217$	$-0.5819 \leq d \leq 0.1327$	$-1.6358 \leq d \leq 0.8384$	$-1.1388 \leq d \leq 2.6816$

Using these relations, we can find the value of e_C for which e_I reaches its maximum value. After obtaining e_I and e_C, we can calculate C_1 and C_5 for the optimal point. This calculation procedure can be converted into a theoretical restriction for the cascade stages: Constant values of C_1 and C_5 for all stages.

THEORETICAL MODELS FOR CASCADE SIMULATION

Combining the $7n$ mass balance relations and $2n$ of the restrictions cited above, we can construct the different mathematical models described below.

1. Cascade with constant cut and constant separation factor (6–11). In this model it is assumed that all stages work with the optimal cut θ_{ot} and the optimal separation factor α_{ot}.
2. Cascade with constant cut and constant C_1 and C_5 theoretical parameters. In this model the cut is assumed to be θ_{ot} for all stages, and the heads or the tails separation factors are calculated using the theoretical relations described above.
3. Cascade with symmetric stages and constant separation factor (11). In this model we assume $\beta_{ot} = \gamma_{ot} = \sqrt{\alpha_{ot}}$ for all stages.
4. Cascade with symmetric stages and constant C_1 and C_5 parameters. In this model we assume $\beta = \gamma$ for all stages, with β or γ calculated using the theoretical relations.
5. Cascade without restrictions of cut or symmetric behavior and constant C_1 and C_5 parameters. In this model we assume that β and γ obey the theoretical relations for all stages.
6. Cascade with symmetric stages and constant centrifuge efficiency. In this model we assume that all the centrifuges operate with the maximum separative power δU_{ot} (efficiency e_{ot}) and in the symmetric process ($\beta = \gamma$).

COMPARISON BETWEEN CALCULATED VALUES AND EXPERIMENTAL RESULTS

Experimental results were obtained using four different cascade configurations with different numbers of enriching and stripping stages, different numbers of centrifuges per stage, and constituted of ultracentrifuges with different internal characteristics operating at their nominal point.

The internal and external flow rates and compositions were calculated for each cascade configuration using the six mathematical models described above.

The relative percentage deviations among the calculated values using each model and the experimental results obtained in each cascade for the external variables are listed in Table 1.

The product and tails abundance ratios (R_p and R_w), the ratios between the product and feed flow rates (P/F), and the separative capacity (ΔU) are compared as external variables.
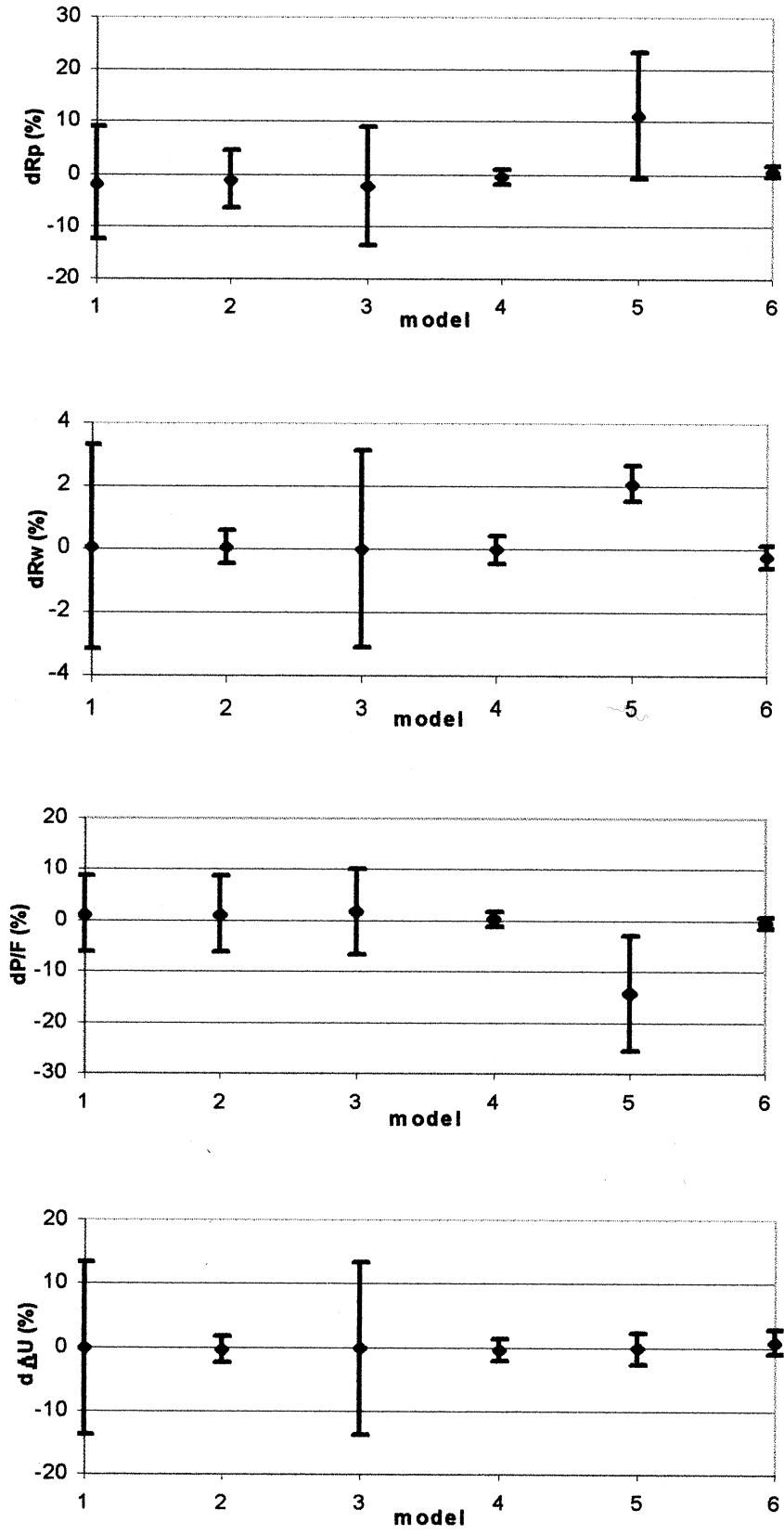
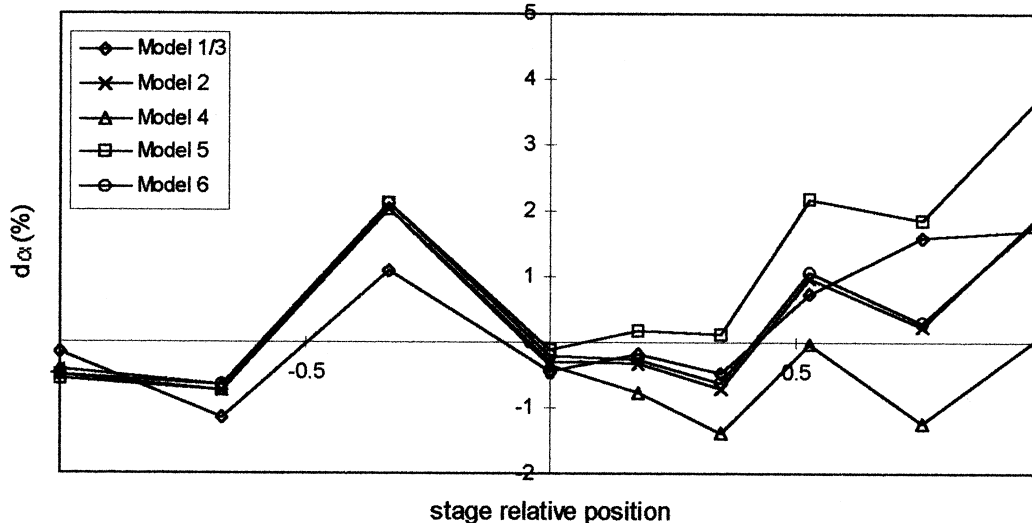FIG. 1   Percentage relative deviation comparison for the external variables.

FIG. 2 Internal separation factors comparison.

With the use of these deviation values for each external variable in each different model, the confidence interval for the real average deviation with a 95% significance level is calculated (12). The results obtained for each model are listed in Table 1 and plotted in Fig. 1.

The separation factors of all stages were experimentally determined for one of the four cascade arrangements as internal variables (Cascade 3). The relative percentage deviations obtained as a function of the relative position of the stages in the enriching and stripping sections of the cascade are shown in Fig. 2. This figure shows we obtained very good results, with small relative percentage deviations for five methods (Models 1, 2, 3, 4, and 6).

By treating the separation factor deviations of all stages as independent variables, we can calculate the average value and the 95% confidence interval for the average deviation for the six different models. The values obtained are shown in Table 2 and plotted in Fig. 3.

TABLE 2
Average Values for Percentage Relative Deviation of the Internal Separation Factors

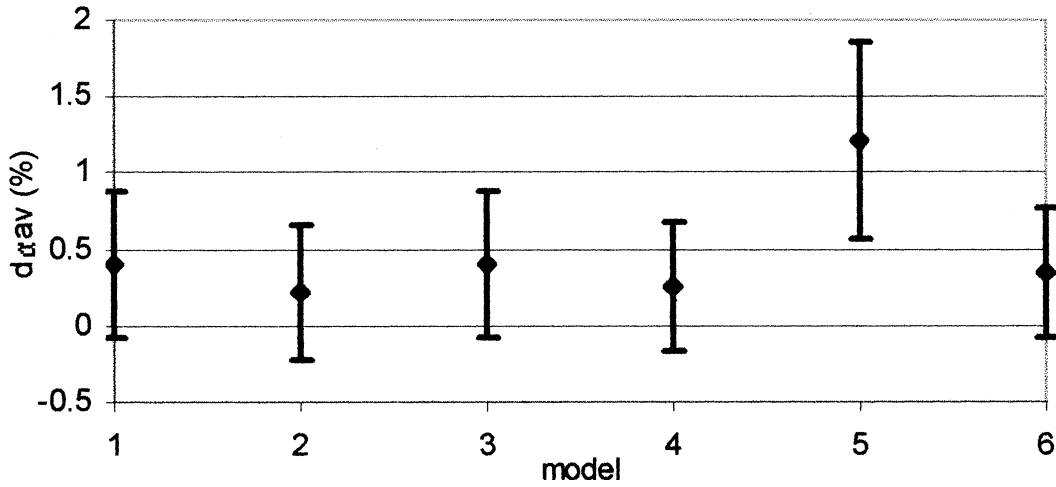| Model	Average deviation	Standard deviation	Confidence interval
1	0.3973	1.0604	$-0.0854 \leq d \leq 0.8800$
2	0.2187	0.9574	$-0.2171 \leq d \leq 0.6545$
3	0.3973	1.0604	$-0.0854 \leq d \leq 0.8800$
4	0.2543	0.9218	$-0.1653 \leq d \leq 0.6739$
5	1.2100	1.4135	$0.5666 \leq d \leq 1.8534$
6	0.3467	0.9284	$-0.0759 \leq d \leq 0.7693$

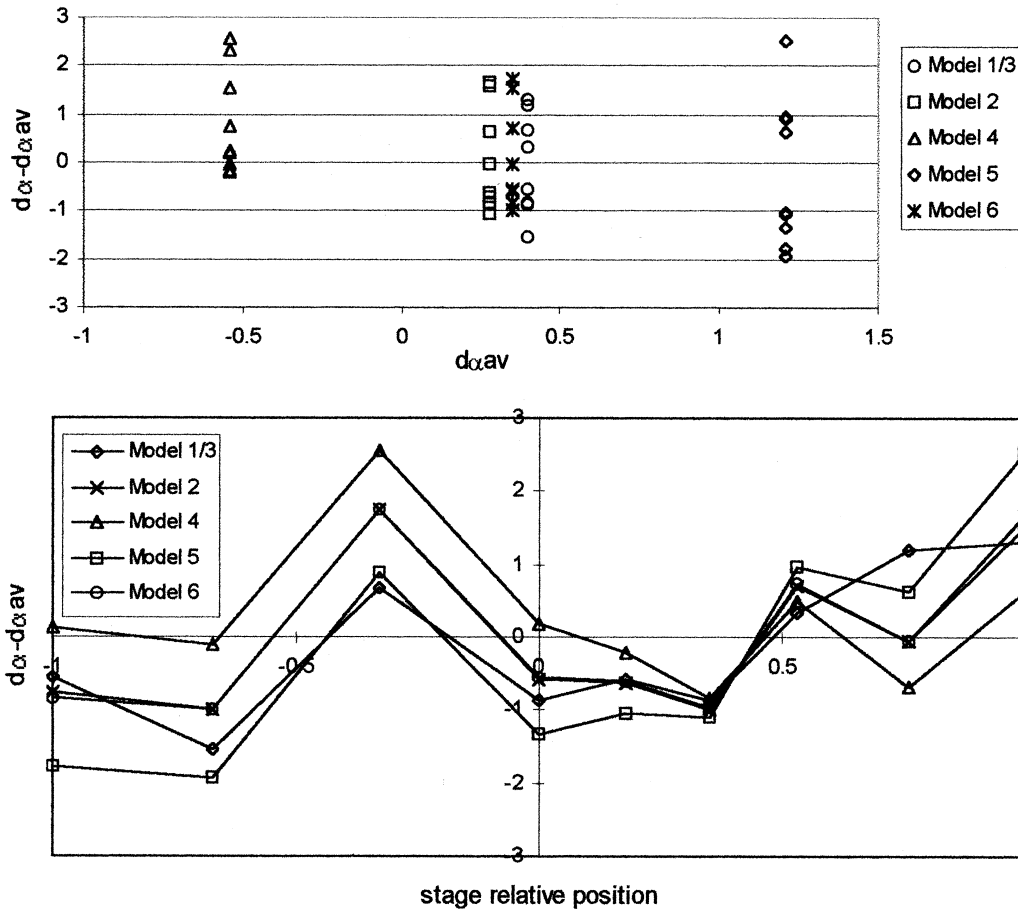FIG. 3   Average internal separation factor percentage relative deviation comparison.

FIG. 4   Residuals analysis.

In order to prove that the internal separation factors can really be treated as independent variables, an analysis of the residuals (12) was executed and the residuals obtained (local value − average value) were plotted as a function of the average value and of the relative position of the cascade stages the enriching and stripping sections. These plots are shown in Fig. 4.

This figure shows that there is nothing in the behavior of the analyzed variable, either relative to the calculated values or relative to the position of the cascade stages, that does not permit the stage separation factors to be treated as independent variables.

CONCLUSIONS

The tables and figures show that the best method for the theoretical simulation of real cascade behavior is one in which all stages are considered to operate in a symmetric process and with maximum separative power (Model 6), followed by Model 4. For Model 6 we obtained the smallest relative percentage deviation between the calculated and measured values for almost all the internal and external variables that were compared. This approximation introduces small errors to the model because of the shape of the $\delta U \times G$ curve in a centrifuge. There is a relatively large feed flow rate interval for which δU is almost constant. This fact permits an internal feed flow rate profile with different values for each stage to be fitted for each cascade without being very far from the real separative power value.

However, we have to keep in mind that all these comparisons and models are completely valid only for cascades designed to operate near the symmetric conditions. If the cascade stages were designed to operate asymmetrically ($\beta \neq \gamma$), the restrictions proposed might be invalid and, depending on the degree of asymmetry, all these analyzed models could fail to simulate the cascade's real behavior.

ACKNOWLEDGMENT

REFERENCES

1. K. Cohen. *The Theory of Isotope Separation as Applied to Large Scale Production of ^{235}U*, McGraw-Hill, New York, NY, 1951.
2. N. Ozaki and I. Harada, "Optimization of the Cascade with Gas Centrifuges for Uranium Enrichment," in *Proceedings of the International Conference of Uranium Isotope Separation*, BNES, London, March 1975.
3. D. R. Olander, "Design of Ideal Cascades of Gas Centrifuges with Variable Separation Factors," *Nucl. Sci. Eng. 60*, 421–434 (1976).

4. R. Canales and D. A. White, "A Generalized Algorithm for Cascade Mass Balances," *Chem. Eng. Sci.*, *48*(4), 819–821 (1993).

5. I. Jordan and J. H. Buchmann, *The Isotopic Separation Theory in a Countercurrent Centrifuge and Separative Parameters Calculation*, IPEN C-5 Publication, July 1983 (in Portuguese).

6. A. Apelblat and Y. Ilamed-Lehrer, "The Theory of a Real Isotope Enriching Cascade—I, II," *J. Nucl. Energy*, *22*, 1–26 (1968).

7. T. Kawai, K. Inoue, H. Motoda, T. Kobayashi, and T. Kiguchi, "Sensitivity Analysis of Ideal Centrifuge Cascade for Producing Slightly Enriched Uranium," *Nucl. Sci. Eng.*, *50*, 63–72 (1973).

8. T. Kiguchi, H. Motoda, and T. Kawai, "Stochastic Fluctuation in a Uranium-Enriching Cascade Using the Centrifuge Process," *Nucl. Technol. 17*(February), 168–183 (1973).

9. E. Von Halle, *Cascade Design Considerations for Cascades Composed of Stages with Large Separation Factors* (K/04-4175), Enrichment Planning Department, Operations Analysis and Planning Division, Oak Ridge Gaseous Diffusion Plant, Oak Ridge, TN, February 1978.

10. T. Kai, "Basic Characteristics of a Low Uranium Enrichment Cascade by Centrifugation (I)," *J. At. Energy Soc. Jpn.*, *17*(1), 31–44 (1975).

11. I. Yamamoto and A. Kanagawa, "Analytical Solution for Real Cascade Equation in Steady State," *J. Nucl. Sci. Technol. 12*(2), 120–127 (1975).

12. G. E. P. Box, W. G. Hunter, and J. S. Hunter, *Statistics for Experimenters*, Wiley, New York, NY, 1978.